Computational Investigation of the Stability of Stenotic Carotid Artery under Pulsatile Blood Flow Using a Fluid-Structure Interaction Approach

Amirhosein Manzoori
Sharif University of Technology
Famida Fallah (fallah@sharif.ir)
Sharif University of Technology https://orcid.org/0000-0003-0884-1560
Mohammadali Sharzehee
University of Texas at San Antonio John Peace Library
Sina Ebrahimi
Sharif University of Technology

Research

Keywords: Stenotic Artery, Artery Buckling, Fluid-Structure Interaction, Buckling Pressure, Pulsatile Flow

Posted Date: May 8th, 2020

DOI: https://doi.org/10.21203/rs.3.rs-25564/v1

Version of Record: A version of this preprint was published at International Journal of Applied Mechanics on December 1st, 2020. See the published version at https://doi.org/10.1142/S1758825120501100.

Abstract

Background

Stenosis can disrupt the normal pattern of blood flow, and thus make the artery more susceptible to buckling which may cause arterial tortuosity. Although the stability simulations of the atherosclerotic arteries were conducted based on solid modelling and static internal pressure, the mechanical stability of stenotic artery under pulsatile blood flow remains unclear while pulsatile nature of blood flow makes the artery more critical for stresses and stability. The aim of this study was to investigate the effect of stenosis on arterial stability under pulsatile blood flow.

Methods

To this end, fluid-structure interaction (FSI) simulations of arteries stenosis under pulsatile flow were conducted. 3D idealized geometries of carotid arteries stenosis with symmetric and asymmetric plaques along with different percentages of stenosis were created. Arterial wall was modelled as an anisotropic hyperelasic material.

Results

It is observed that the stenosis percentage, symmetry/asymmetry of the plaque, and the stretch ratio can dramatically affect the buckling pressure. Buckling makes the plaque rupture (especially in asymmetric ones) more likely due to increasing the stresses on it. The dominant stresses on plaques are the circumferential, axial and radial ones, respectively. Also, the highest shear stresses on the plaques were detected in $\theta - z$ and $r - \theta$ planes for the symmetric and asymmetric stenotic arteries, respectively. In addition, the maximum circumferential stress on the plaques was observed in the outer point of the buckled configuration for symmetric and asymmetric stenosis as well as at the ends of the asymmetric plaque. Furthermore, the artery buckling caused a large vortex flow at the downstream of the plaque. As a result, the conditions for the penetration of lipid particles and the formation of new plaques were provided.

Conclusion

Buckling makes the plaque rupture more likely due to increasing the stresses on it especially in asymmetric plaques. In addition, the artery buckling provides the condition for the penetration of lipid particles and the formation of new plaques at the downstream of the plaque.

Full Text

Tables

Due to technical limitations, Table 1 is provided in the Supplentary Files section.

Figures

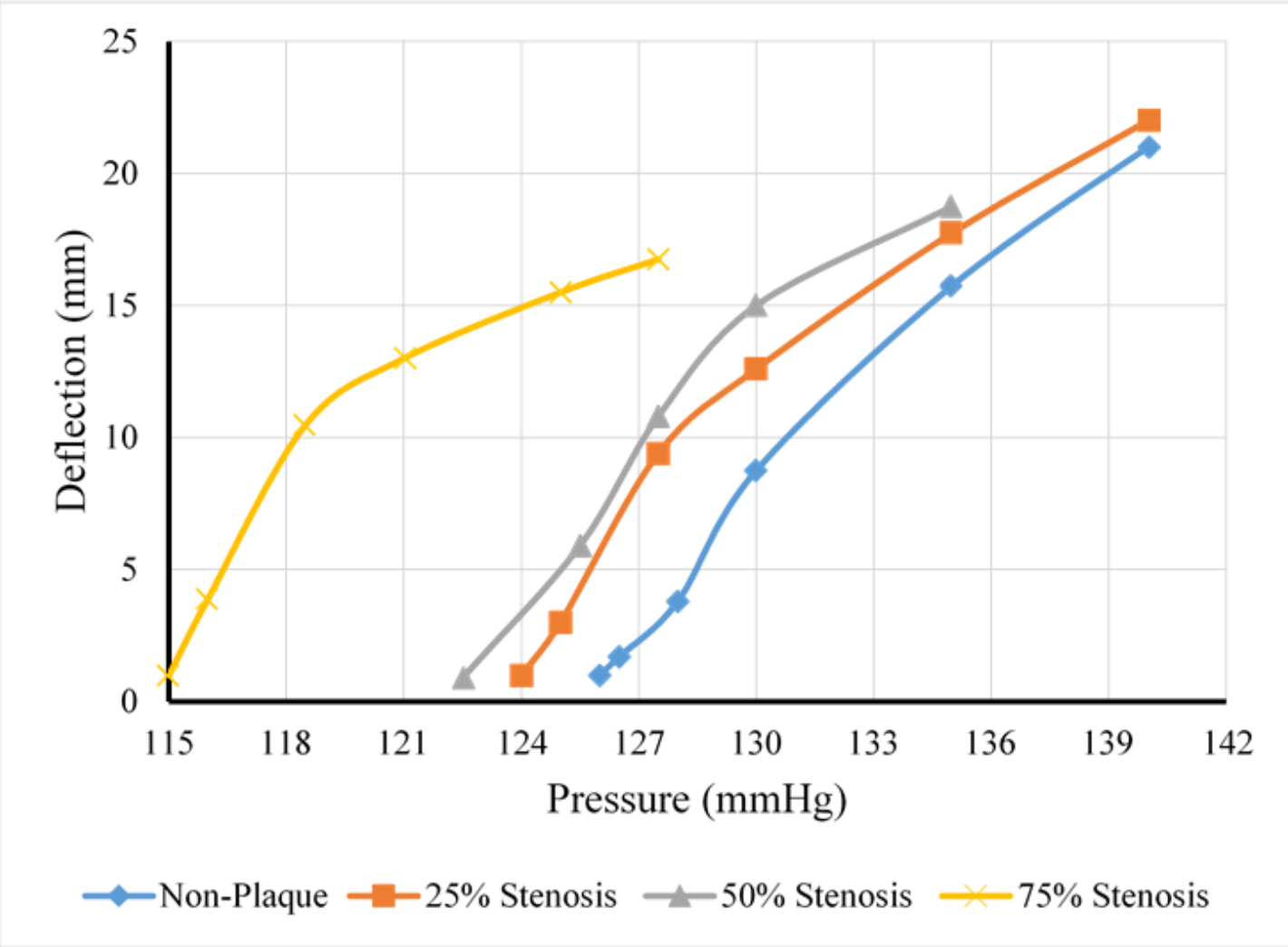

Figure 1

Maximum post-buckling deflection of normal and stenotic arteries with symmetric plaques against the mean pressure in stretch ratios of 1.5.

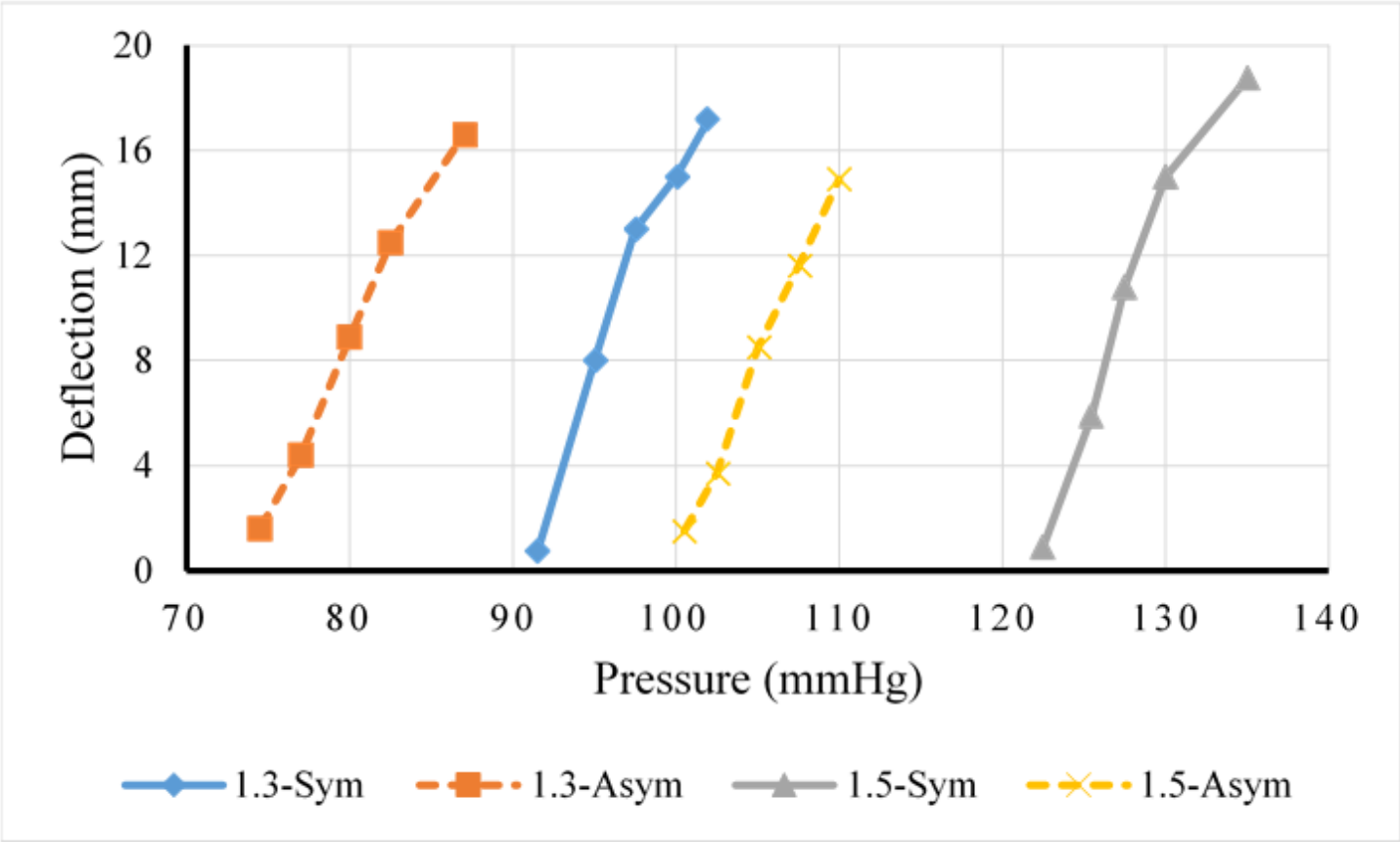

Figure 2

Maximum post-buckling deflection of 50% stenotic arteries with symmetric and asymmetric plaques against the mean pressure in stretch ratios of 1.3 and 1.5.

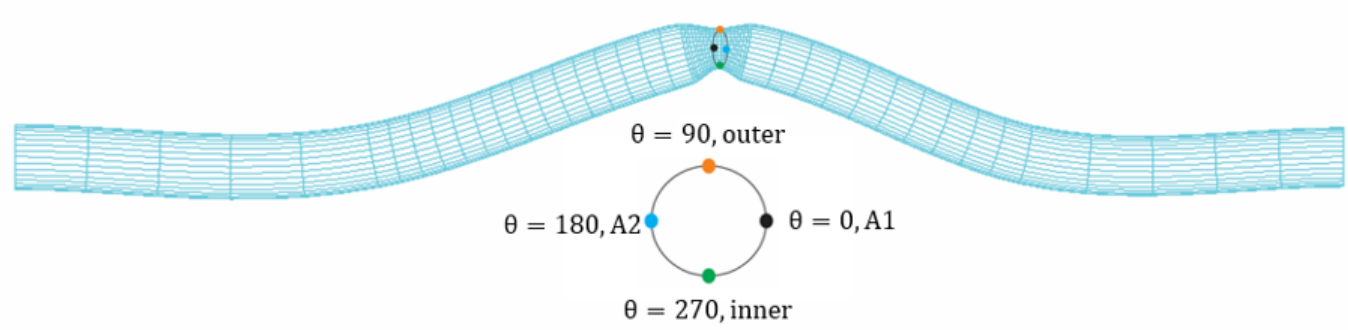

Figure 3

Schematic of the outer, inner, A1, and A2 points

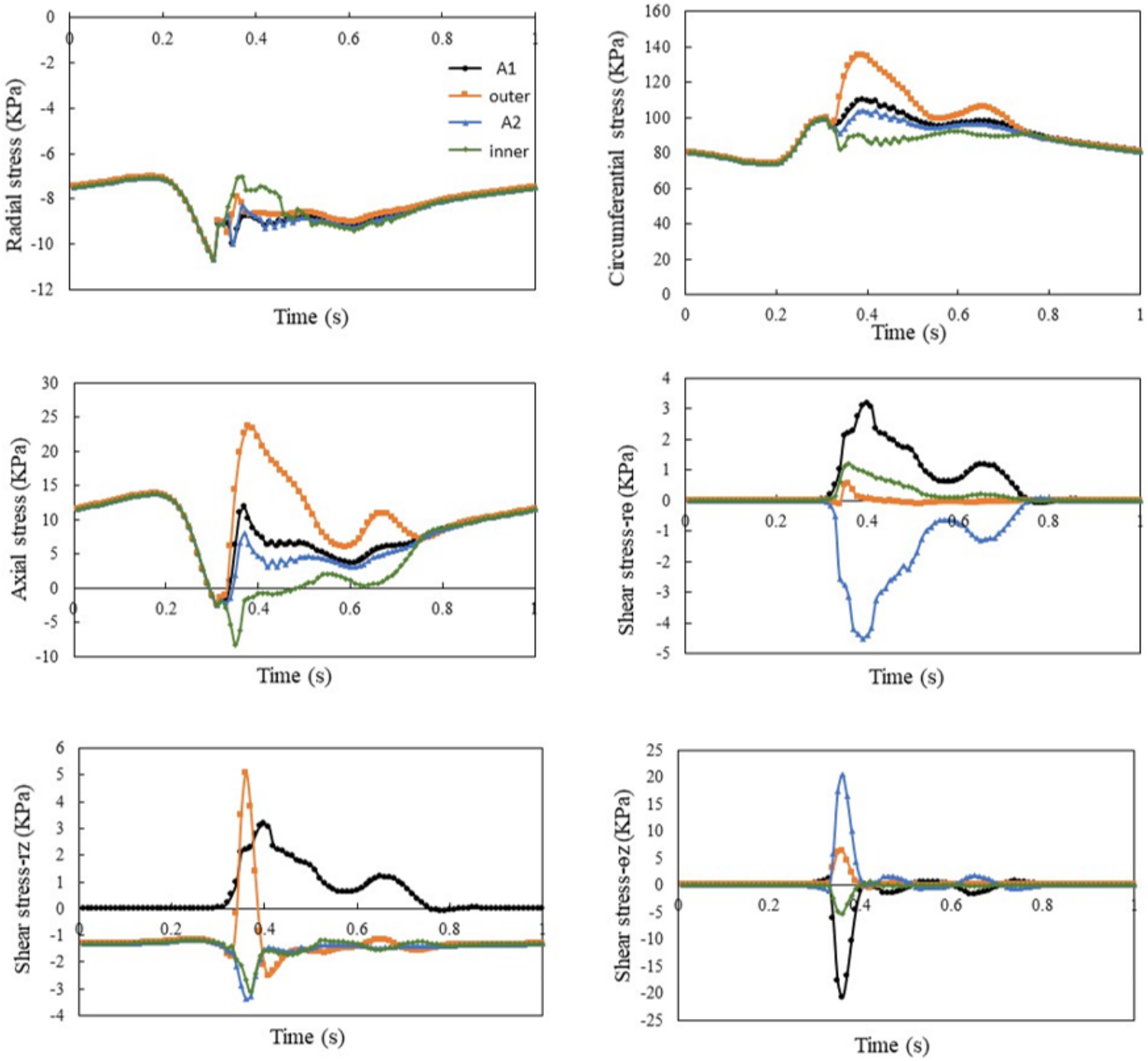

Figure 4

Temporal variations of all stress components on the plaque at the inner, outer, A1, and A2 points in the stenotic artery with 50% symmetric plaque under mean pressure of 102 mmHg and axial stretch ratio of 1.3.

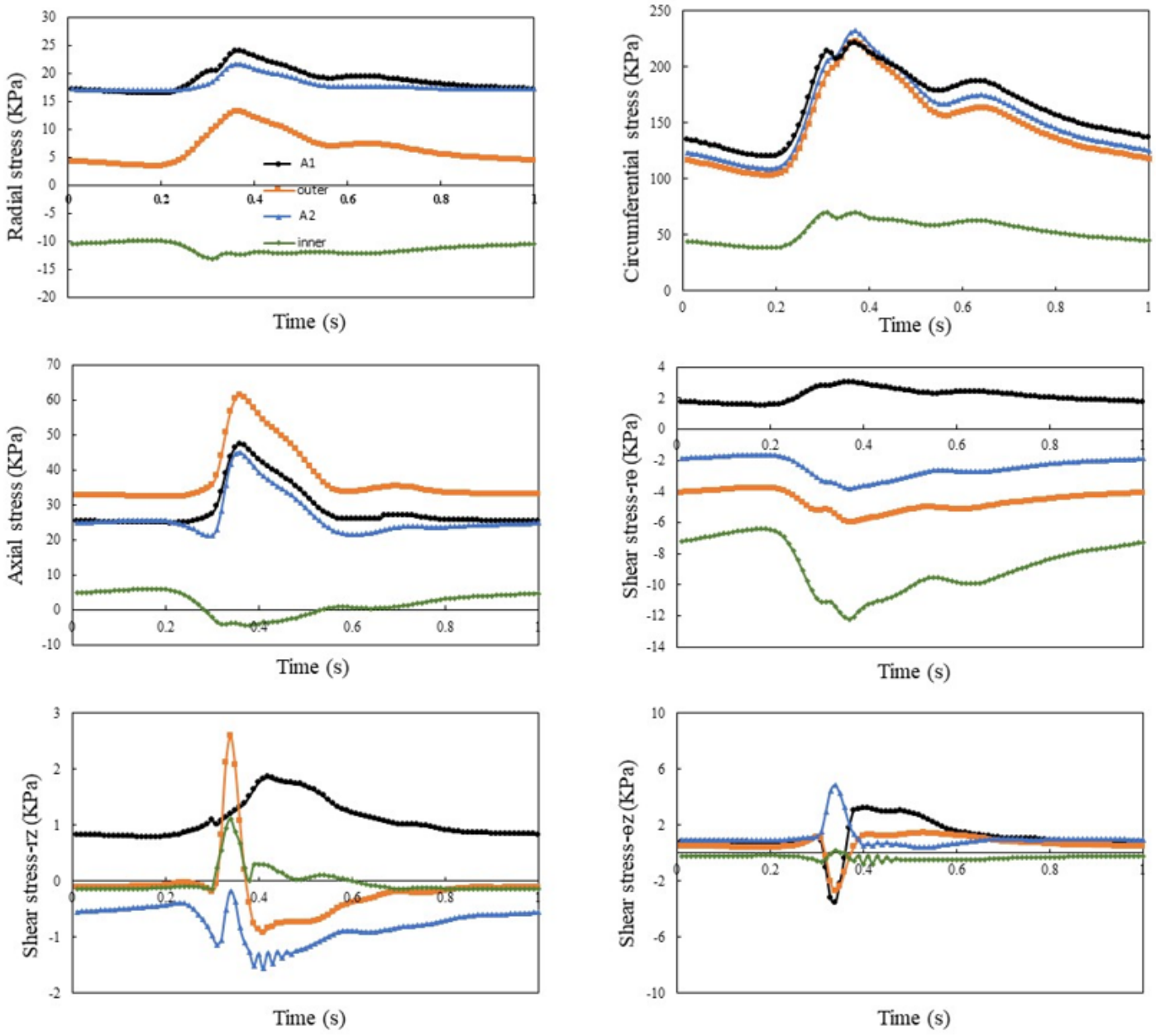

Figure 5

Temporal variations of all stress componenst on the plaque at the inner, outer, A1, and A2 points in the stenotic artery with 50% asymmetric plaque under mean pressure of 87 mmHg and axial stretch ratio of 1.3.

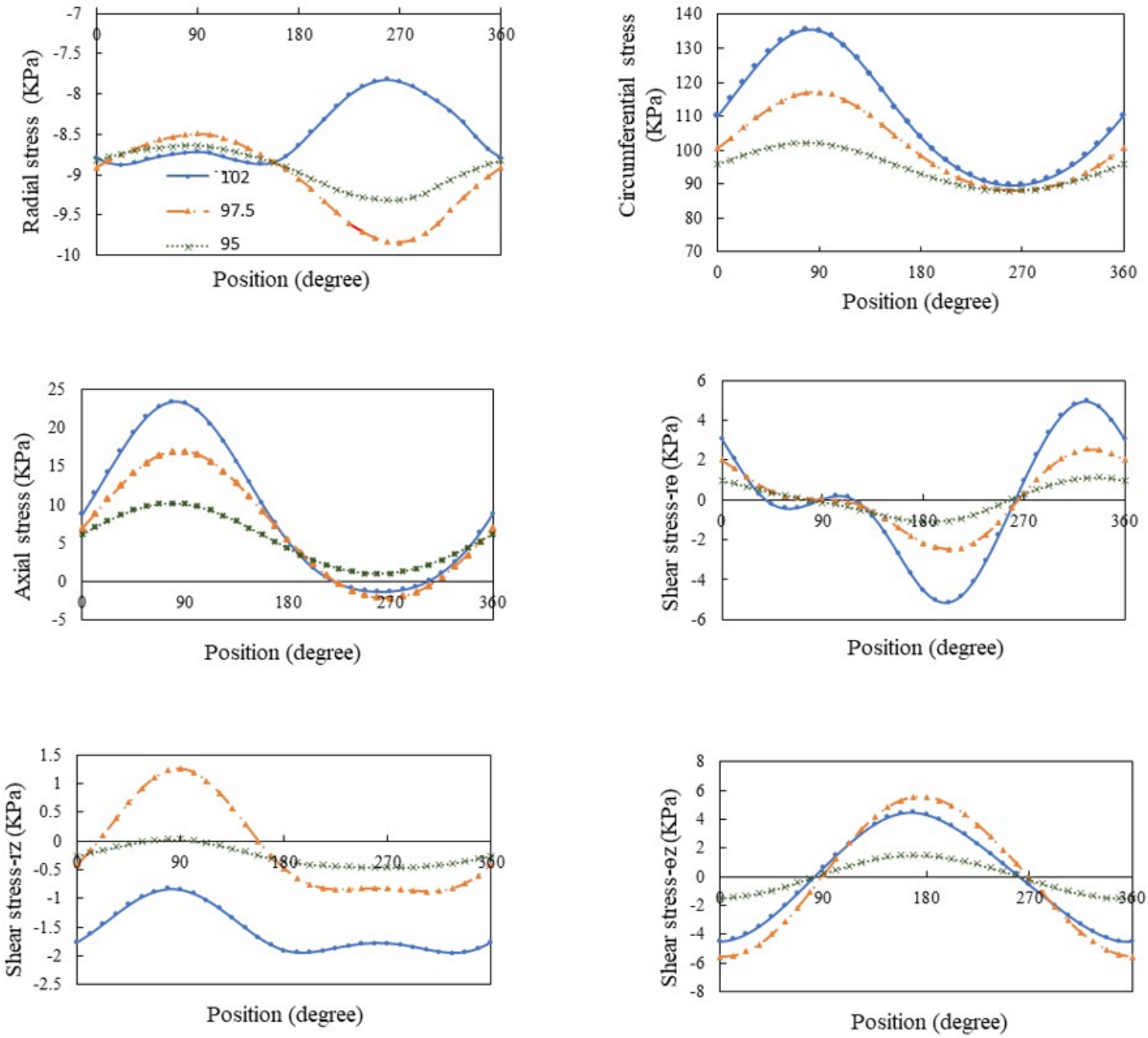

Figure 6

Circumferential distribution of all stress components on the plaque at the moment of peak deflection in the stenotic artery with 50% symmetric plaque with stretch ratio of 1.3 and mean pressures of 95, 97.5 and 102 mmHg.

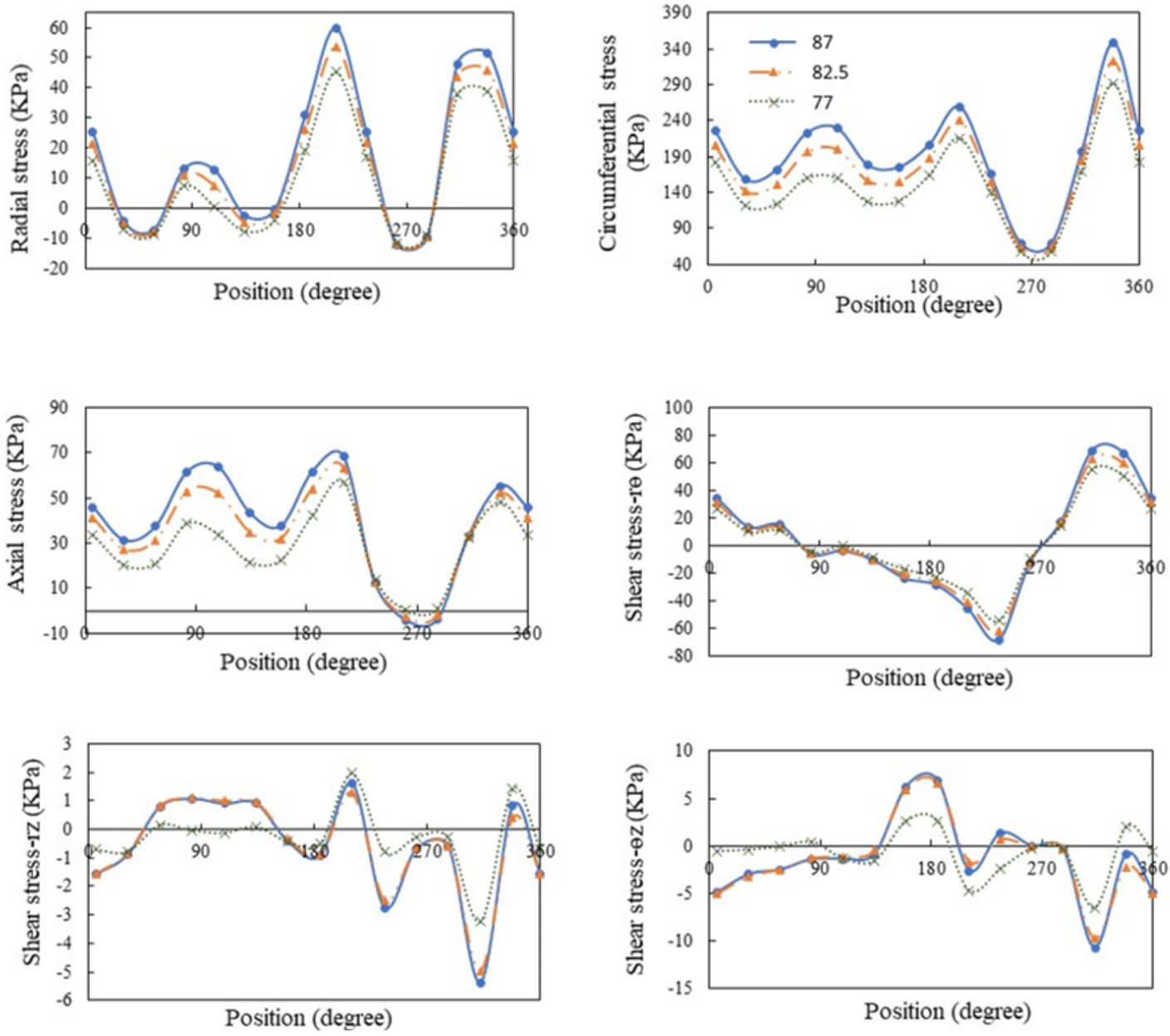

Figure 7

Circumferential distribution of all stress components on the plaque at the peak deflection in the stenotic artery with 50% asymmetric plaque with stretch ratio of 1.3 and mean pressures of 77, 82.5 and 87 mmHg.

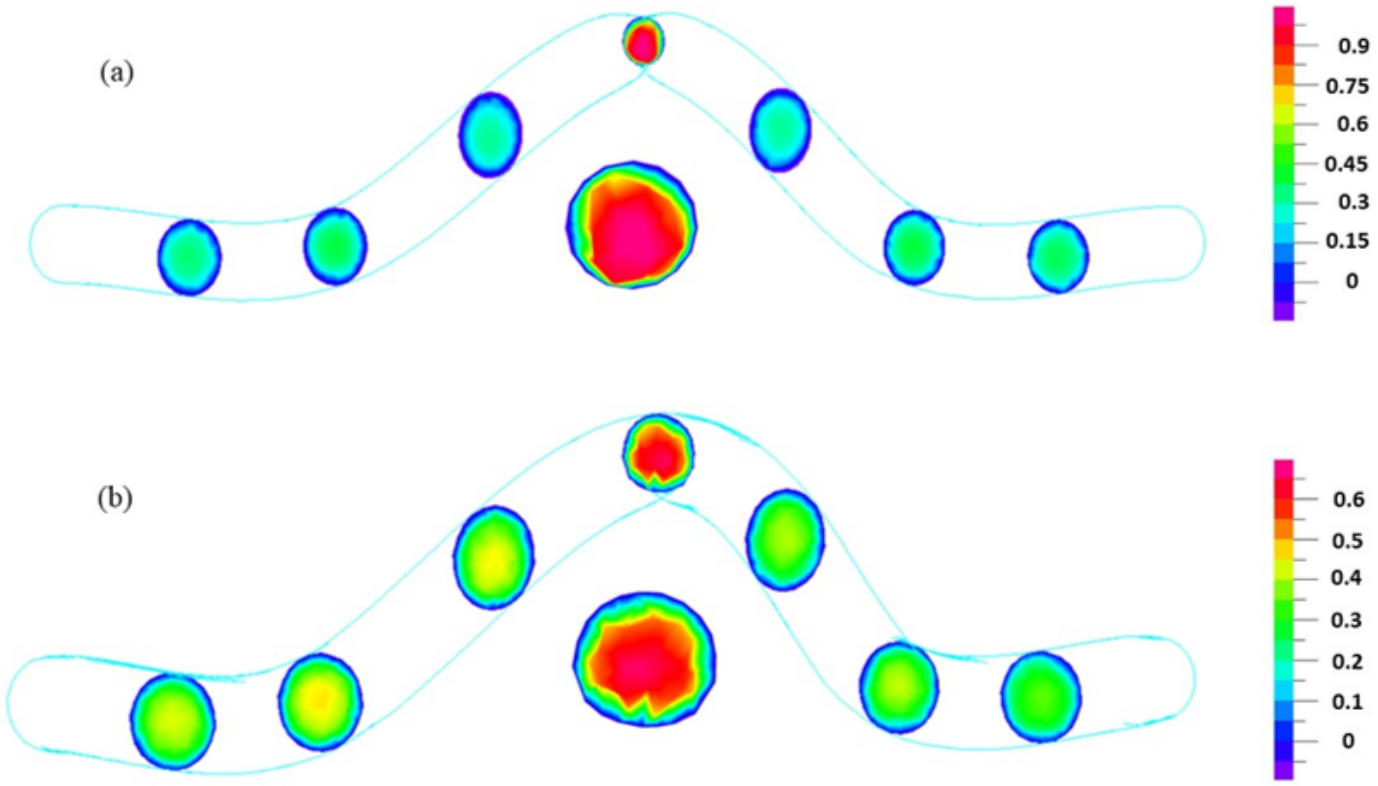

Figure 8

Velocity contour (m/s) at the peak deflection (a) for stenotic artery with 50% symmetric plaque with mean pressure of 102 mmHg (b) for stenotic artery with 50% asymmetric plaque with mean pressure of 87 mmHg

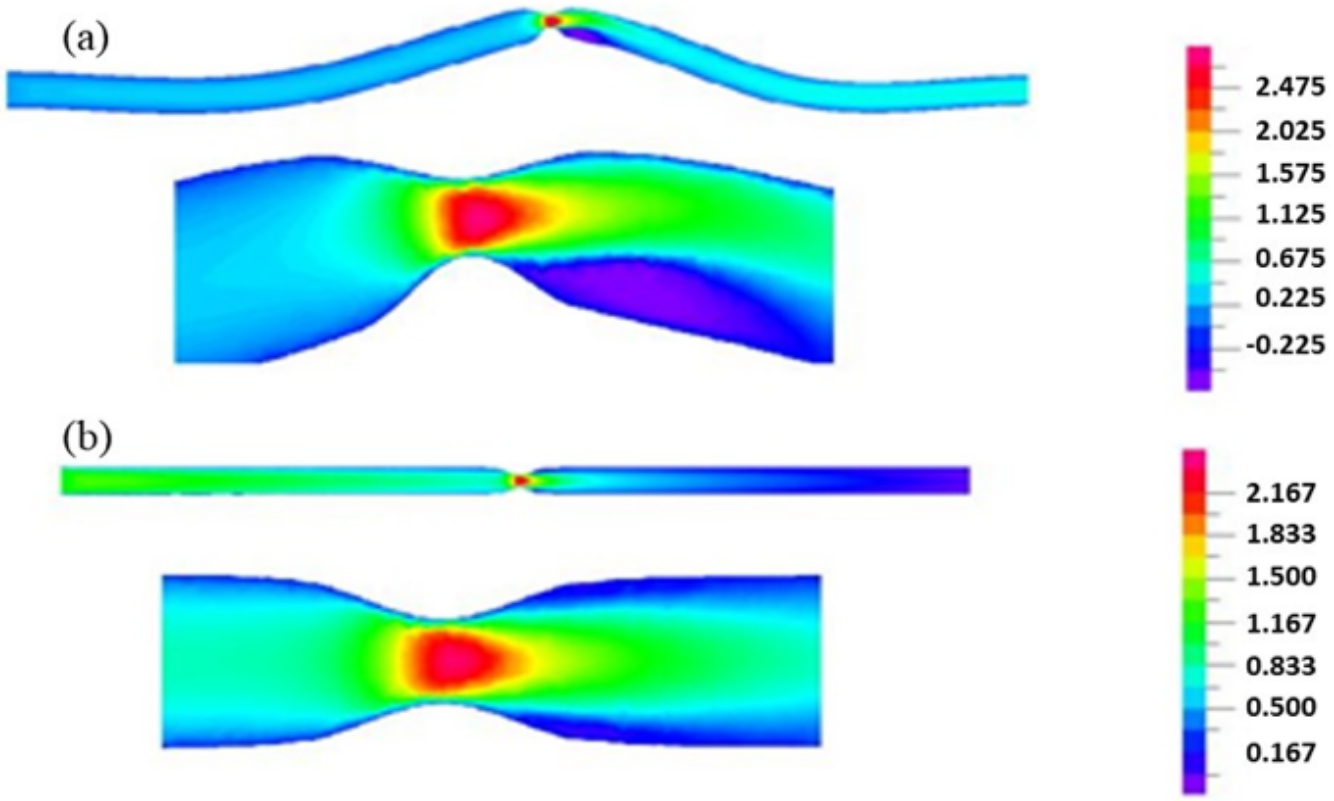

Figure 9

Velocity contour (m/s) in the stenotic artery with 75% plaque under a stretch ratio of 1.3 and a mean pressure of (a) 90 mmHg for symmetric plaque and (b) 85 mmHg for asymmetric plaque

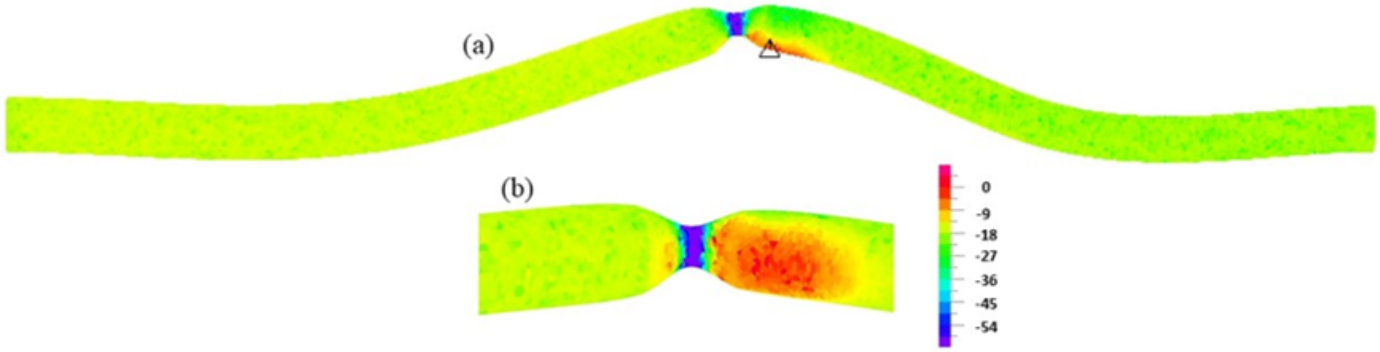

Figure 10

(a) Contour of lumen shear stress (Pa) for stenotic artery with 75% symmetric plaque under a mean pressure of 90 mmHg and a stretch ratio of 1.3 (b) Magnified view of the area with the minimum shear stress.

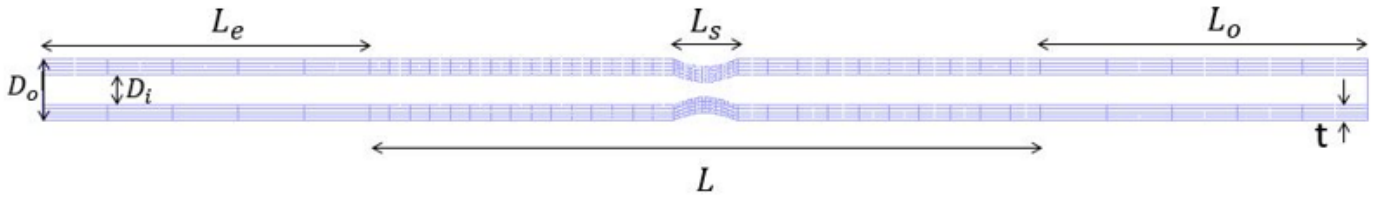

Figure 11

Dimensions of artery with 75% symmetric plaque in a longitudinal cross section

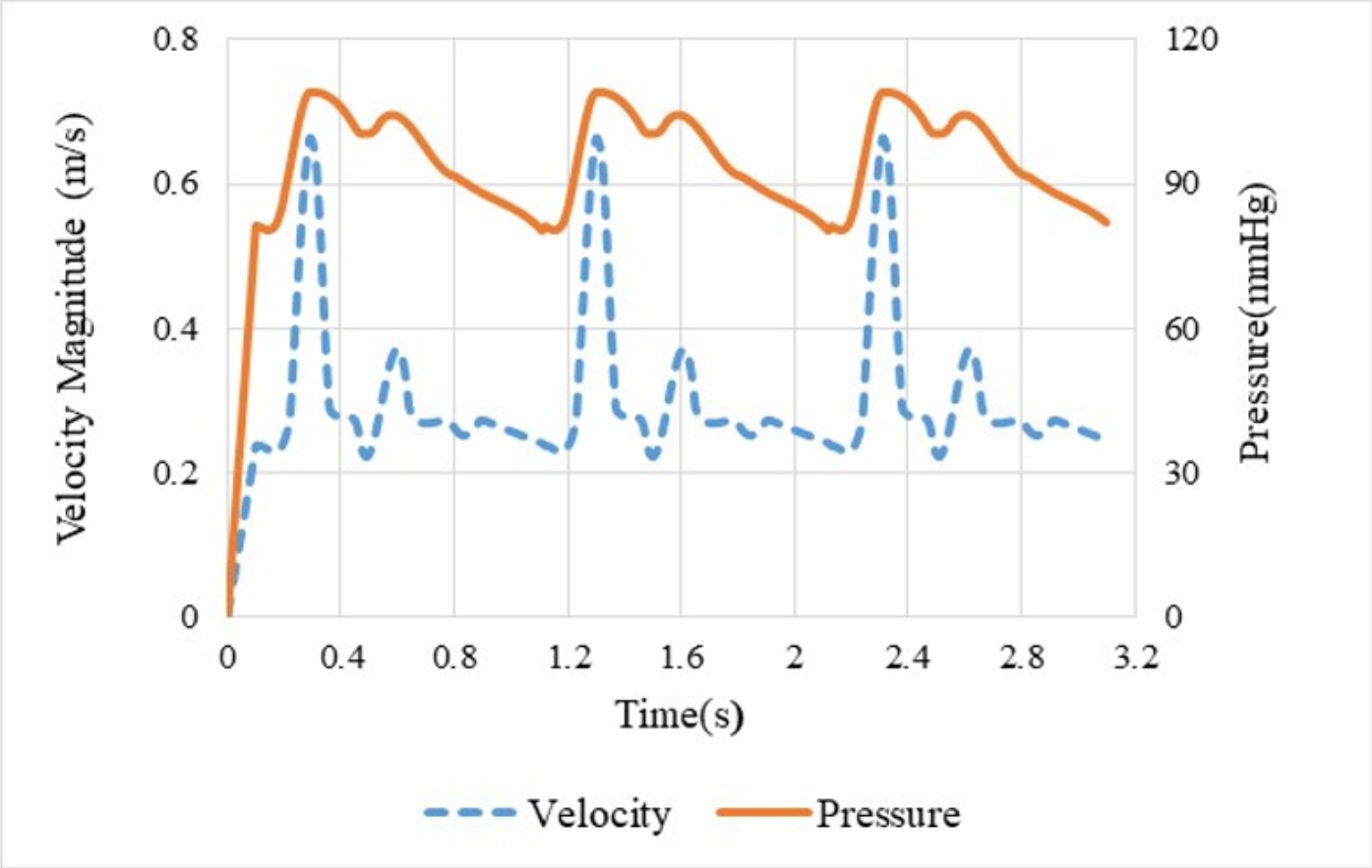

Figure 12

Pulsatile inlet velocity and outlet pressure in the carotid artery for three cardiac cycles.

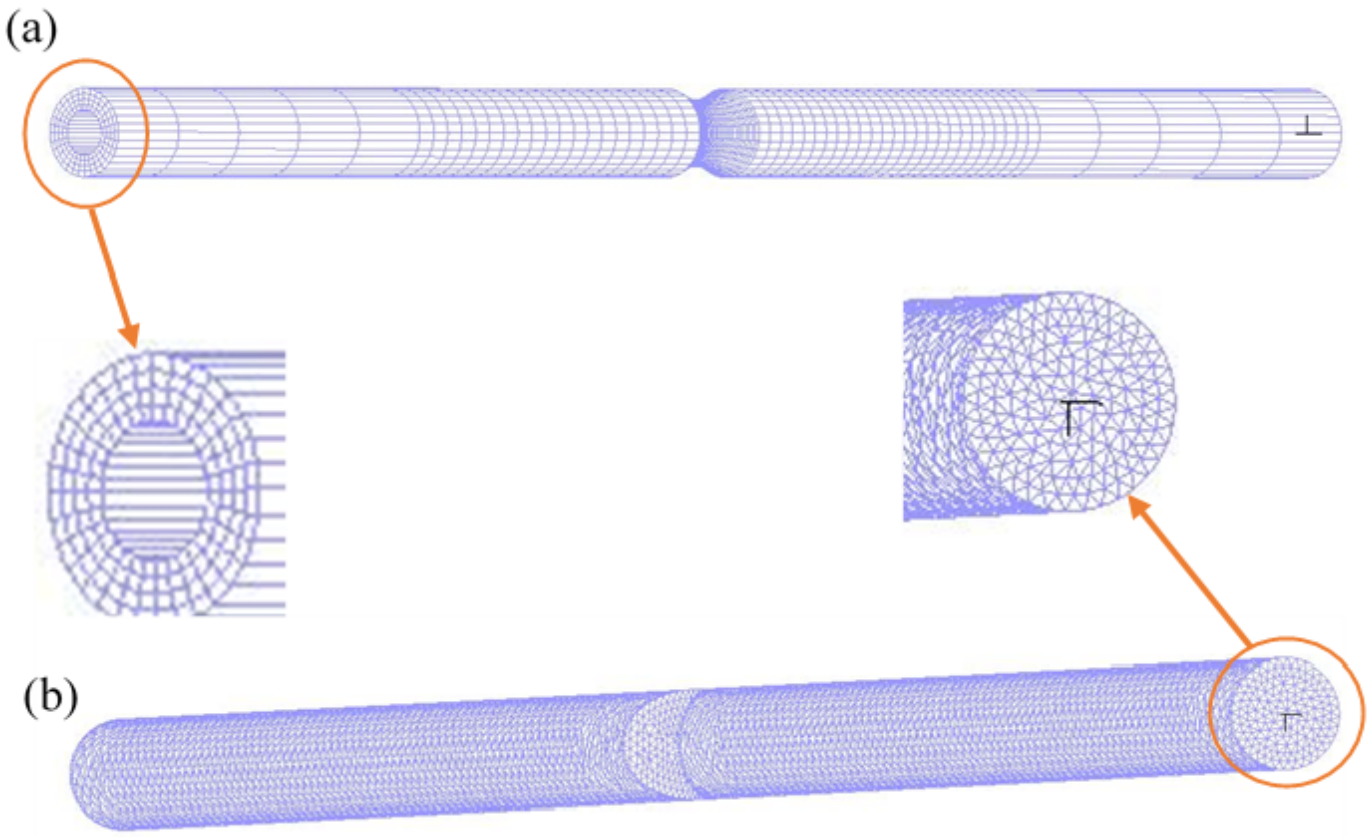

Figure 13

(a) Solid domain mesh in arteries with symmetric stenosis of 75% and (b) fluid domain mesh in arteries with asymmetric stenosis of 75%.